

# Negative Currents in Fabry-Pérot Cavities are Caused by Interfering Paths

Mrinmoyee Saha, Luca Horray, Pedro Portugal, and Christian Flindt  
*Department of Applied Physics, Aalto University, 00076 Aalto, Finland*

The time-dependent electric current in a Fabry-Pérot cavity can turn negative even if the time-dependent voltage is always positive. Here we present an analytic theory of this surprising phenomenon, showing that it is a purely quantum mechanical effect. It only occurs at low temperatures, and it is caused by interferences between paths through the cavity with different numbers of round trips. We provide realistic parameters for observing the negative currents in an experiment and show that a similar phenomenon is expected for the heat current, which may also turn negative.

*Introduction*—Gigahertz voltage pulses have paved the way for experiments in high-frequency quantum transport, where just a single or a few electronic excitations are emitted into a mesoscopic conductor [1–3]. Lorentzian pulses generate clean single-particle excitations known as levitons, which can be controlled and manipulated as photons in quantum optics [4–9]. When emitted close to the Fermi level, these excitations interact only weakly. By contrast, recent collision experiments have revealed strong interactions between high-energy excitations that arrive simultaneously on each side of a beam splitter [10–12]. Moreover, by increasing the driving frequency and shortening the pulse duration, many dynamical phenomena may soon be discovered [13, 14].

At low temperatures, electronic excitations can experience quantum coherence over an entire mesoscopic structure, such that interference effects become observable. A prominent example is the Hong-Ou-Mandel effect [15, 16], which recently was realized with electrons [7–9]. In addition, Mach-Zehnder interferometers and Fabry-Pérot cavities have been implemented with mesoscopic circuits [17–19]. While these devices have mainly been explored using static voltages, several theoretical predictions have been made for setups driven by voltage pulses [1–3, 20, 21]. For instance, advanced numerical simulations have shown that the time-dependent electric current in a Fabry-Pérot cavity may turn negative, although the time-dependent voltage is always positive [22, 23]. This surprising prediction may soon be within experimental reach, and it is therefore a timely task to develop a theoretical description of the underlying physics. Here, we show that the negative currents arise from a dynamical interference effect, which is somewhat similar to how quantum interference can lead to negative probabilities in full counting statistics. [24].

In this Letter, we present an analytic theory of negative currents in mesoscopic Fabry-Pérot cavities driven by voltage pulses as illustrated in Fig. 1(a). To this end, we use Floquet scattering theory to show that the negative currents are caused by interferences between scattering paths through the cavity with different numbers of round trips. The negative currents are a purely quantum mechanical effect, which gets washed out by an increasing temperature as shown in Fig. 1(b). Our theoretical

description allows us to provide realistic parameter estimates for observing negative currents in future experiments. We also extend our analysis to the heat current by showing that a similar interference effect can cause the heat current to turn negative. As such, our work illustrates how dynamic interference effects may soon be observable in high-frequency transport experiments.

*Fabry-Pérot cavity*— Figure 1(a) shows an electronic Fabry-Pérot cavity made up of two quantum point contacts that are separated by the distance  $L$ . We can write the transmission amplitude of the device as a sum over

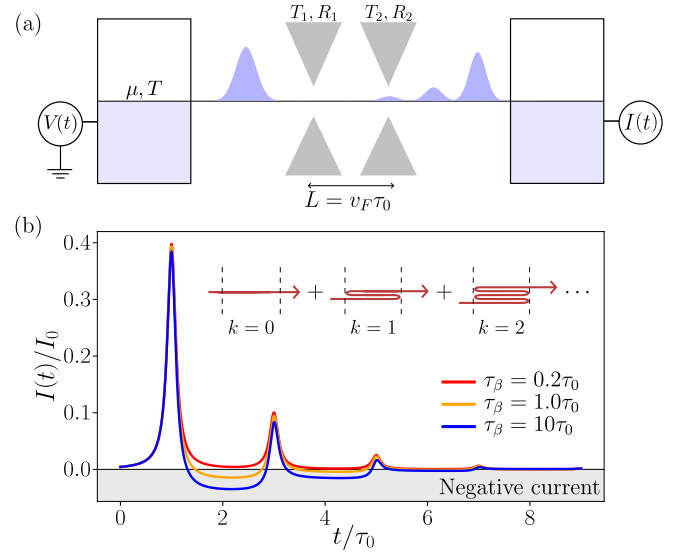


FIG. 1. Negative currents in a Fabry-Pérot cavity. (a) The device consists of two quantum point contacts with transmission and reflection probabilities  $T_{1,2}$  and  $R_{1,2}$ , separated by the distance  $L$ . Electrons travel at the Fermi velocity  $v_F$ . (b) Time-dependent electric current in response to a Lorentzian voltage pulse of halfwidth  $\Gamma = 0.1\tau_0$ , which excites an average charge of  $q = 0.5$  electrons. In all figures, the transmission and reflection probabilities are  $T_{1,2} = R_{1,2} = 1/2$ , and we have defined  $I_0 = e/\tau_0$ . We show results for different temperatures given by the thermal timescale  $\tau_\beta = \hbar/\pi k_B T$ . The transmission amplitude in Eq. (1) is the sum over all scattering paths from the source to the drain with  $k = 0, 1, 2, \dots$  round trips inside the cavity, here with  $\varphi = \pi/3$ .

all possible scattering paths through the cavity,

$$t(E) = t_1 t_2 e^{iE\tau_0/\hbar} \sum_{k=0}^{\infty} \left[ r_1 r_2 e^{i(2E\tau_0/\hbar + \varphi)} \right]^k, \quad (1)$$

where  $\tau_0 = L/v_F$  is the time it takes to travel between the quantum point contacts, with transmission and reflection amplitudes  $t_{1,2}$  and  $r_{1,2}e^{i\varphi_{1,2}}$ , at the Fermi velocity  $v_F$  [25]. Here, we have taken the transmission amplitudes to be real without loss of generality, while  $\varphi = \varphi_1 + \varphi_2$  is the phase that is picked up upon reflections on both quantum point contacts. This phase may also account for an enclosed magnetic flux or a shift of the chemical potential in the electrodes. With a constant voltage, the current through the interferometer is determined by the transmission function  $T(E) = |t(E)|^2$ . By contrast, if driven by voltage pulses, the current depends on the transmission amplitude at two different energies, and there will be products of amplitudes corresponding to paths with different numbers of round trips, leading to interferences and negative currents, as we will see.

We now consider voltage pulses that are applied to the source, while the time-dependent current is measured in the drain. To be specific, we consider Lorentzian voltage pulses, but one can also analyze other time-dependent voltages. The sequence of Lorentzian pulses reads

$$eV(t) = \frac{q\hbar\Omega}{\pi} \sum_n \frac{\Gamma\mathcal{T}}{\Gamma^2 + (t - n\mathcal{T})^2}, \quad (2)$$

where  $\Omega = 2\pi/\mathcal{T}$  is the driving frequency, and  $\mathcal{T}$  is the period. The halfwidth of the pulses is denoted by  $\Gamma$ , and  $q$  is the average charge excited by each pulse. To evaluate the electric current, we make use of Floquet scattering theory and thus consider the scattering phase due to the voltage,  $\mathcal{J}(t) = \exp\{-i\phi(t)\}$  with  $\phi(t) = e \int_{-\infty}^t dt' V(t')/\hbar$  [26–28]. Its Fourier components,  $\mathcal{J}_n = \int_0^{\mathcal{T}} dt \mathcal{J}(t) e^{in\Omega t}/\mathcal{T}$ , are the amplitudes for an electron in the source to change its energy from  $E$  to  $E_n = E + n\hbar\Omega$  by exchanging  $n$  modulation quanta with the drive. Since the pulses are generated indepen-

dently of the cavity, the Floquet scattering matrix becomes  $S_n(E) = t(E_n)\mathcal{J}_n$ , which includes the transmission amplitude for an excited electron to reach the drain.

*Electric current*— The electric current now reads [26]

$$I(t) = \frac{e}{h} \int_{-\infty}^{\infty} dE \sum_{m,n} S_n^*(E) S_m(E) \mathcal{F}_n(E) e^{i\Omega t(n-m)}, \quad (3)$$

where  $\mathcal{F}_n(E) = f_S(E) - f_D(E_n)$  is the difference of the Fermi functions in the source and the drain. The electrodes have the same temperature  $T$  and chemical potential  $\mu = 0$ , such that  $f_S(E) = f_D(E) = f(E)$ .

To evaluate the current, we consider the product

$$S_n^*(E) S_m(E) = \mathcal{J}_n^* \mathcal{J}_m T_1 [T_{\text{cl}} + T_{\text{int}}(E)] T_2 e^{i\Omega\tau_0(n-m)}, \quad (4)$$

which we have split into two terms by defining

$$T_{\text{cl}} = \sum_{k=0}^{\infty} \left[ R_2 R_1 e^{i2\Omega\tau_0(n-m)} \right]^k, \quad (5)$$

where  $T_{1,2} = t_{1,2}^2$  and  $R_{1,2} = r_{1,2}^2$ , and

$$T_{\text{int}}(E) = \sum_{k \neq l}^{\infty} (r_2 r_1)^{k+l} e^{i2\Omega\tau_0(ml-nk)} e^{i2E\tau_0(l-k)/\hbar} e^{i2\varphi k}. \quad (6)$$

The current corresponding to the first term then becomes  $I_{\text{cl}}(t) = T_1 T_2 \sum_{k=0}^{\infty} (R_2 R_1)^k I_{\text{in}}(t - \tau_k)$ , where  $I_{\text{in}}(t) = (e^2/h)V(t)$  is the current from the source, and  $\tau_k = (2k+1)\tau_0$  is the time it takes to complete  $k+1/2$  round trips inside the cavity. Here, we have used that  $T_{\text{cl}}$  is energy independent, such that the integral in Eq. (3) becomes  $\int_{-\infty}^{\infty} dE \mathcal{F}_n(E) = n\hbar\Omega$ . We can then perform the sums as  $\sum_n n\hbar\Omega \mathcal{J}_n e^{-i\Omega t n} = -i\hbar\partial_t \mathcal{J}(t)$  and  $\sum_m \mathcal{J}_m e^{-i\Omega t m} = \mathcal{J}(t)$  and use that  $i\hbar[\partial_t \mathcal{J}(t)]^* \mathcal{J}(t) = eV(t)$ .

Evaluating the current corresponding to the second term is more involved, since  $T_{\text{int}}(E)$  is energy-dependent. However, using the integral in Eq. (11) of the End Matter, we eventually find the total current, which becomes

$$I(t) = T_1 T_2 \sum_{k=0}^{\infty} (R_2 R_1)^k \left\{ (e^2/h)V(t - \tau_k) + 2e \sum_{l=1}^{\infty} (r_2 r_1)^l \chi(\tau_{l-1/2}/\tau_\beta) \text{Re} \left[ e^{i(2l-1)\varphi} G^{(1)}(t - \tau_k, t - \tau_{k+l}) \right] \right\}, \quad (7)$$

where the temperature enters the function  $\chi(x) = x/\sinh(x)$  through the thermal time scale  $\tau_\beta = \hbar/\pi k_B T$  [29, 30]. This time scale determines how long particles can travel before the interferences are lost. We

have also introduced the correlation function [31]

$$G^{(1)}(t, t') = \frac{\exp\{-i\phi(t, t')\} - 1}{2\pi i(t - t')}, \quad (8)$$

having used that  $\mathcal{J}^*(t)\mathcal{J}(t') = \exp\{-i\phi(t, t')\}$ , where  $\phi(t, t') = \phi(t') - \phi(t) = e \int_t^{t'} ds V(s)/\hbar$ .

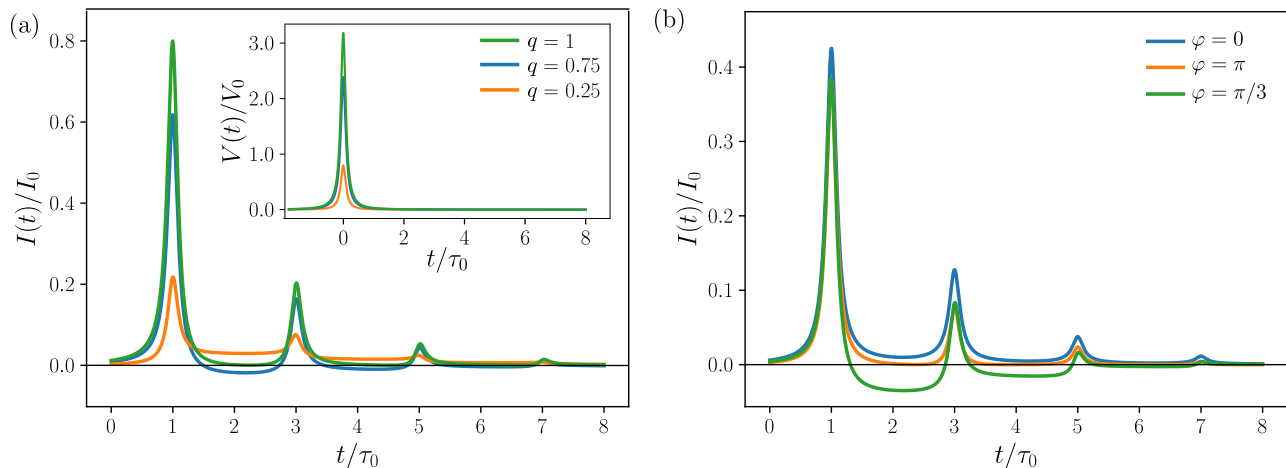


FIG. 2. Negative electric currents. (a) Time-dependent electric current corresponding to the Lorentzian voltage pulse in the inset with halfwidth  $\Gamma = 0.1\tau_0$  and average charge  $q$ . Both the temperature and the flux are zero. The period of the drive is so large that we can consider the effect of just a single pulse. Here, we have defined  $V_0 = h/e\tau_0$ , and  $I_0 = e/\tau_0$ . (b) Time-dependent electric current at zero temperature for different phases and pulses with an average charge of  $q = 0.5$  electrons.

Equation (7) constitutes a central result of this Letter, and it explains the occurrence of negative currents. At high temperatures, where  $\tau_\beta \ll \tau_0$ , we have  $\chi \simeq 0$ , such that the second term in the curly brackets vanishes, and we are left with the first term. This term corresponds to classical expectations, where the injected charge bounces back and forth between the quantum point contacts, before it eventually reaches the drain. By contrast, at low temperatures, where  $\chi \simeq 1$ , the second term becomes important. This term describes interferences between paths through the cavity with a difference of round trips given by the integer  $l$ , and it can make the current negative. The period of the drive does not explicitly appear in Eq. (7), and we can take it to be so long that we can evaluate the current in response to just a single pulse.

*Negative electric currents*— In Figs. 1(b) and 2, we show the electric current calculated for Lorentzian voltage pulses based on Eq. (7). The period is so large that the current corresponds to the single voltage pulse shown in the inset of Fig. 2(a), where we consider three different values of the average charge excited by the pulse. In both figures, the electric current turns negative at certain times, and in Fig. 1(b), we see how the negative current goes away as the temperature is increased, which destroys the interferences. As such, the negative currents are a dynamic quantum effect. In Fig. 2(b), we show the electric current for different phases, which can be used to control the sign of the current according to Eq. (7).

*Experimental considerations*— To provide realistic estimates for observing the negative currents, we note that temperatures of  $T = 20$  mK are reachable in state-of-the-art experiments, corresponding to a thermal time scale of about  $\tau_\beta \simeq 100$  ps. Taking conservative estimates such as a Fermi velocity of  $v_F = 10^5$  m·s<sup>-1</sup> and a distance

of  $L = 500$  nm between the quantum point contacts, we find  $\tau_0 = 5$  ps  $\ll \tau_\beta$ , which is sufficiently short to maintain phase coherence. These numbers can be further improved by reducing the distance between the quantum point contacts, so that a quantum dot effectively is formed [32]. Of course, the interferences can be destroyed by other mechanisms than a finite electronic temperature, and an observation of negative currents may require a highly controlled and ultraclean sample. However, if negative currents are measured in an experiment, our theory demonstrates that they are caused by interferences between different scattering paths through the cavity.

*Heat current*— One might think that the negative currents arise because electrons and holes in a pulse propagate differently through the interferometer. Indeed, the negative currents do not occur for Lorentzian pulses with integer charge, where only electrons are excited. However, as we now will see, also the heat current may turn negative, although electrons and holes carry the same amount of heat. In addition, the heat current may turn negative for Lorentzian pulses with integer charge.

The heat current can be expressed as [33, 34]

$$J(t) = \sum_{n,m} \int_{-\infty}^{\infty} \frac{dE}{h} E_{m+\frac{n}{2}} S_n^*(E) S_m(E) \mathcal{F}_{m+\frac{n}{2}}(E) e^{-i(m-n)\Omega t}, \quad (9)$$

which again can be evaluated based on Eq. (4). Since  $T_{cl}$  is energy-independent, the corresponding heat current becomes  $J_{cl}(t) = T_1 T_2 \sum_{k=0}^{\infty} (R_2 R_1)^k J_{in}(t - \tau_k)$ , where  $J_{in}(t) = (e^2/2h) V^2(t) = I_{in}(t) V(t)/2$  is the heat current that would run without the interferometer [35]. Evaluating the heat current corresponding to  $T_{int}(E)$  is again involved because of the energy dependence. However, using the integrals in Eqs. (11) and (12) of the End Matter,

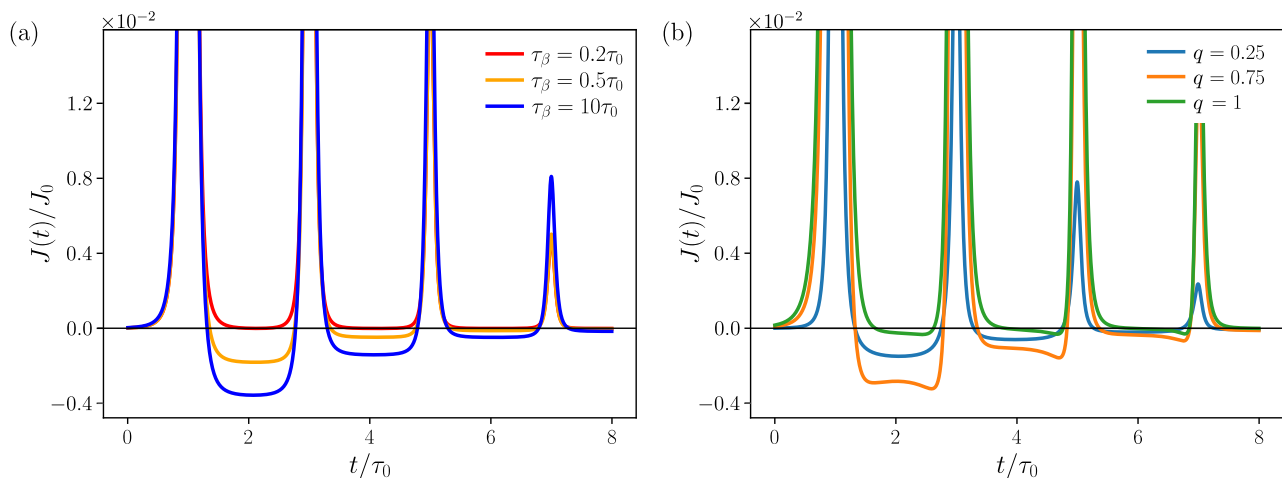


FIG. 3. Negative heat currents. (a) Time-dependent heat current for different temperatures given by the thermal timescale  $\tau_\beta = \hbar/\pi k_B T$  and zero flux. The Lorentzian voltage pulses have the halfwidth  $\Gamma = 0.1\tau_0$  and an average charge of  $q = 0.5$  electrons. The period of the drive is so large that we can consider the effect of just a single pulse, and we have defined  $J_0 = I_0 V_0$  with  $V_0 = \hbar/e\tau_0$  and  $I_0 = e/\tau_0$ . (b) Heat current at zero temperature for different pulses with an average charge of  $q$ .

the total heat current becomes

$$\begin{aligned}
 J(t) = & T_1 T_2 \sum_{k=0}^{\infty} (R_2 R_1)^k \left\{ (e^2/2h) V^2(t - \tau_k) + 2\hbar \sum_{l=1}^{\infty} (r_2 r_1)^l \frac{\gamma(\tau_{l-1/2}/\tau_\beta)}{\tau_l} \text{Im} \left[ G^{(1)}(t - \tau_k, t - \tau_{k+l}) \right] \right\} \\
 & + e T_1 T_2 \sum_{k=0}^{\infty} \sum_{l \neq k}^{\infty} (r_2 r_1)^{l+k} \chi(\tau_{l-k-1/2}/\tau_\beta) \text{Re} \left[ G^{(1)}(t - \tau_k, t - \tau_l) \right] [V(t - \tau_l) + V(t - \tau_k)] / 2,
 \end{aligned} \tag{10}$$

where we have defined the function  $\gamma(x) = \chi^2(x) \cosh(x)$  and set the phase to zero to keep the result simple.

*Negative heat currents*— In Fig. 3, we show the time-dependent heat current for the Lorentzian voltage pulses in Eq. (2), here with a large period. In both panels, the heat current turns negative at certain times, and in Fig. 3(a), we see how the negative currents go away as the temperature is increased. In Fig. 3(b), we show the heat current for different average charges carried by the pulses, and we see that the heat current turns slightly negative also for pulses with integer charge that carry no holes [34, 35]. As such, the negative currents do not occur because electrons and holes propagate differently through the cavity. Rather, they arise because of dynamical interferences between scattering paths through the cavity with a different number of round trips.

*Other pulses*— So far, we have focused on Lorentzian pulses; however, our analytic expressions apply equally well to other voltage pulses. As an example, we show results in the End Matter for Gaussian pulses, which were considered in the earlier numerical simulations [22, 32]. For the Gaussian pulses, we also find negative electric currents and negative heat currents. Moreover, for the

electric current, our analytic expression in Eq. (7) agrees well with the numerical simulations of Ref. [22].

*Conclusions*— We have presented a theory of negative currents in Fabry-Pérot cavities, which shows that they are rooted in interferences between scattering paths through the device with different numbers of round trips. The negative currents are a purely quantum mechanical effect, which gets washed away by an increasing temperature. Realistic estimates indicate that negative currents may be observable in future experiments on high-frequency quantum transport. To this end, our analytic expressions for the currents may be used to optimize the pulses to achieve the most negative currents. Here, we have considered a mesoscopic Fabry-Pérot cavity made up of two quantum point contacts; however, our predictions also apply to other similar interferometers, for instance, an NIS (normal-metal/insulator/superconductor) junction, where the insulating layer and the superconductor both function as reflecting mirrors [36]. Our work also has implications for the field of quantum thermodynamics regarding the currents that flow and the work that is performed because of an external driving field [37].

*Acknowledgments*— We thank P. Buset, M. Kari,

J. Kotilahti, M. Moskalets, and B. Roussel for useful discussions and acknowledge the support from the Finnish doctoral school in Quantum Science and Technology and Research Council of Finland through the Finnish Centre of Excellence in Quantum Technology (grant number 352925) and the Finnish Quantum Flagship.

- 
- [1] E. Bocquillon, V. Freulon, F. D. Parmentier, J.-M. Berroir, B. Plaçais, C. Wahl, J. Rech, T. Jonckheere, T. Martin, C. Grenier, D. Ferraro, P. Degiovanni, and G. Fève, Electron quantum optics in ballistic chiral conductors, *Ann. Phys.* **526**, 1 (2014).
- [2] J. Splettstoesser and R. J. Haug, Single-electron control in solid state devices, *Phys. Status Solidi B* **254**, 1770217 (2017).
- [3] C. Bäuerle, D. C. Glattli, T. Meunier, F. Portier, P. Roche, P. Roulleau, S. Takada, and X. Waintal, Coherent control of single electrons: a review of current progress, *Rep. Prog. Phys.* **81**, 056503 (2018).
- [4] L. S. Levitov, H. Lee, and G. B. Lesovik, Electron counting statistics and coherent states of electric current, *J. Math. Phys.* **37**, 4845 (1996).
- [5] D. A. Ivanov, H. W. Lee, and L. S. Levitov, Coherent states of alternating current, *Phys. Rev. B* **56**, 6839 (1997).
- [6] J. Keeling, I. Klich, and L. S. Levitov, Minimal Excitation States of Electrons in One-Dimensional Wires, *Phys. Rev. Lett.* **97**, 116403 (2006).
- [7] J. Dubois, T. Jullien, F. Portier, P. Roche, A. Cavanna, Y. Jin, W. Wegscheider, P. Roulleau, and D. C. Glattli, Minimal-excitation states for electron quantum optics using levitons, *Nature* **502**, 659 (2013).
- [8] T. Jullien, P. Roulleau, B. Roche, A. Cavanna, Y. Jin, and D. C. Glattli, Quantum tomography of an electron, *Nature* **514**, 603 (2014).
- [9] A. Assouline, L. Pugliese, H. Chakraborti, S. Lee, L. Bernabeu, M. Jo, K. Watanabe, T. Taniguchi, D. C. Glattli, N. Kumada, H.-S. Sim, F. D. Parmentier, and P. Roulleau, Emission and coherent control of Levitons in graphene, *Science* **382**, 1260 (2023).
- [10] J. Wang, H. Edlbauer, A. Richard, S. Ota, W. Park, J. Shim, A. Ludwig, A. D. Wieck, H.-S. Sim, M. Urdampilleta, T. Meunier, T. Kodera, N.-H. Kaneko, H. Sellier, X. Waintal, S. Takada, and C. Bäuerle, Coulomb-mediated antibunching of an electron pair surfing on sound, *Nat. Nanotech.* **18**, 721 (2023).
- [11] J. D. Fletcher, W. Park, S. Ryu, P. See, J. P. Griffiths, G. A. C. Jones, I. Farrer, D. A. Ritchie, H.-S. Sim, and M. Kataoka, Time-resolved Coulomb collision of single electrons, *Nat. Nanotech.* **18**, 727 (2023).
- [12] N. Ubbelohde, L. Freise, E. Pavlovska, P. G. Silvestrov, P. Recher, M. Kokainis, G. Barinovs, F. Hohls, T. Weimann, K. Pierz, and V. Kashcheyevs, Two electrons interacting at a mesoscopic beam splitter, *Nat. Nanotech.* **18**, 733 (2023).
- [13] M. Aluffi, T. Vasselon, S. Ouacel, H. Edlbauer, C. Geffroy, P. Roulleau, D. C. Glattli, G. Georgiou, and C. Bäuerle, Ultrashort Electron Wave Packets via Frequency-Comb Synthesis, *Phys. Rev. Appl.* **20**, 034005 (2023).
- [14] S. Ouacel, L. Mazzella, T. Kloss, M. Aluffi, T. Vasselon, H. Edlbauer, J. Wang, C. Geffroy, J. Shaju, A. Ludwig, A. D. Wieck, M. Yamamoto, D. Pomaranski, S. Takada, N.-H. Kaneko, G. Georgiou, X. Waintal, M. Urdampilleta, H. Sellier, and C. Bäuerle, Electronic interferometry with ultrashort plasmonic pulses, [arXiv:2408.13025](https://arxiv.org/abs/2408.13025) (2025).
- [15] C. K. Hong, Z. Y. Ou, and L. Mandel, Measurement of subpicosecond time intervals between two photons by interference, *Phys. Rev. Lett.* **59**, 2044 (1987).
- [16] E. Bocquillon, V. Freulon, J.-M. Berroir, P. Degiovanni, B. Plaçais, A. Cavanna, Y. Jin, and G. Fève, Coherence and Indistinguishability of Single Electrons Emitted by Independent Sources, *Science* **339**, 1054 (2013).
- [17] W. Liang, M. Bockrath, D. Bozovic, J. H. Hafner, M. Tinkham, and H. Park, Fabry-Perot interference in a nanotube electron waveguide, *Nature* **411**, 665 (2001).
- [18] Y. Ji, Y. Chung, D. Sprinzak, M. Heiblum, D. Mahalu, and H. Shtrikman, An electronic Mach-Zehnder interferometer, *Nature* **422**, 415 (2003).
- [19] N. Ofek, A. Bid, M. Heiblum, A. Stern, V. Umansky, and D. Mahalu, Role of interactions in an electronic Fabry-Perot interferometer operating in the quantum Hall effect regime, *Proc. Natl. Acad. Sci.* **107**, 5276 (2010).
- [20] P. Burset, J. Kotilahti, M. Moskalets, and C. Flindt, Time-domain spectroscopy of mesoscopic conductors using voltage pulses, *Adv. Quant. Technol.* **2**, 1900014 (2019).
- [21] J. Kotilahti, P. Burset, M. Moskalets, and C. Flindt, Multi-Particle Interference in an Electronic Mach-Zehnder Interferometer, *Entropy* **23**, 736 (2021).
- [22] B. Gaury and X. Waintal, Dynamical control of interference using voltage pulses in the quantum regime, *Nat. Commun.* **5**, 3844 (2014).
- [23] B. Gaury, J. Weston, M. Santin, M. Houzet, C. Groth, and X. Waintal, Numerical simulations of time-resolved quantum electronics, *Phys. Rep.* **534**, 1 (2014).
- [24] P. P. Hofer and A. A. Clerk, Negative Full Counting Statistics Arise from Interference Effects, *Phys. Rev. Lett.* **116**, 013603 (2016).
- [25] G. B. Lesovik and I. A. Sadovskyy, Scattering matrix approach to the description of quantum electron transport, *Phys.-Usp.* **54**, 1007 (2011).
- [26] M. V. Moskalets, *Scattering Matrix Approach to Non-Stationary Quantum Transport* (Imperial College Press, 2011).
- [27] J. Dubois, T. Jullien, C. Grenier, P. Degiovanni, P. Roulleau, and D. C. Glattli, Integer and fractional charge Lorentzian voltage pulses analyzed in the framework of photon-assisted shot noise, *Phys. Rev. B* **88**, 085301 (2013).
- [28] K. Brandner, Coherent Transport in Periodically Driven Mesoscopic Conductors: From Scattering Amplitudes to Quantum Thermodynamics, *Z. Naturforsch. A* **75**, 483 (2020).
- [29] H.-P. Breuer and F. Petruccione, *The Theory of Open Quantum Systems* (Oxford University Press, 2002).
- [30] H. F. Song, S. Rachel, C. Flindt, I. Klich, N. Laflorencie, and K. Le Hur, Bipartite fluctuations as a probe of many-body entanglement, *Phys. Rev. B* **85**, 035409 (2012).
- [31] M. Moskalets, First-order correlation function of a stream of single-electron wave packets, *Phys. Rev. B* **91**, 195431 (2015).

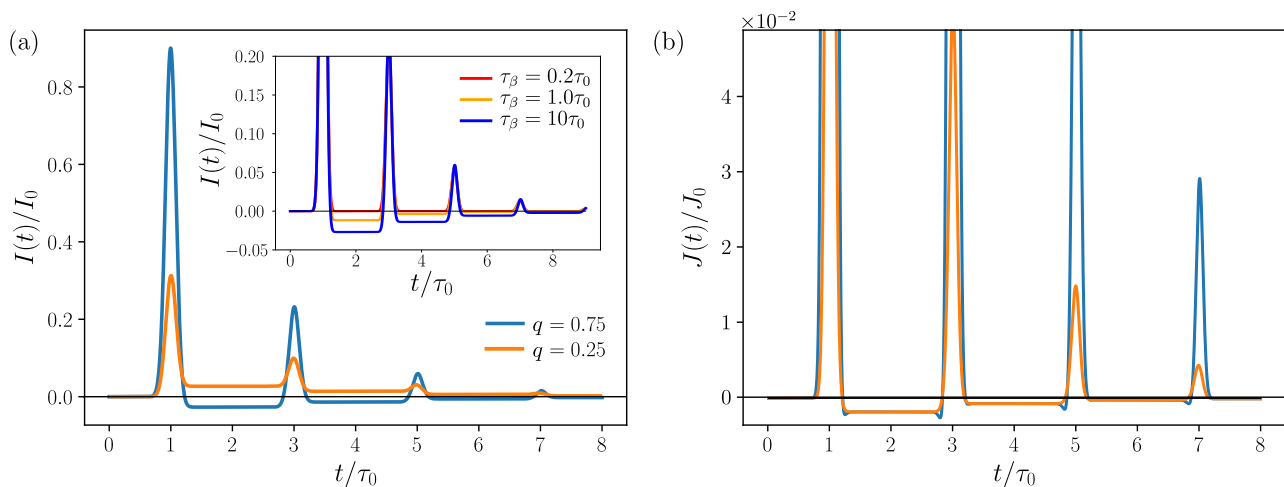


FIG. 4. Negative currents for Gaussian pulses. (a) Electric current at zero temperature and zero phase for the Gaussian pulse in Eq. (13) with  $\Gamma = 0.1\tau_0$  and average charge  $q$ . The inset shows the electric current for different temperatures given by the thermal timescale  $\tau_\beta = \hbar/\pi k_B T$  for pulses with an average charge of  $q = 0.75$  electrons. (b) Time-dependent heat current corresponding to the results in panel (a). Here, we have defined  $I_0 = e/\tau_0$  and  $J_0 = I_0 V_0$  with  $V_0 = \hbar/e\tau_0$ .

- (2015).
- [32] T. Kloss and X. Waintal, Propagation of ultra-short voltage pulses through a small quantum dot, [arXiv:2502.03428](#).
- [33] M. Moskalets and M. Büttiker, Floquet scattering theory for current and heat noise in large amplitude adiabatic pumps, *Phys. Rev. B* **70**, 245305 (2004).
- [34] M. Moskalets and G. Haack, Heat and charge transport measurements to access single-electron quantum characteristics, *Phys. Status Solidi (b)* **254**, 1600616 (2017).
- [35] M. F. Ludovico, J. S. Lim, M. Moskalets, L. Arrachea, and D. Sánchez, Time resolved heat exchange in driven quantum systems, *J. Phys.: Conf. Ser.* **568**, 052017 (2014).
- [36] B. Roussel, P. Buset, and C. Flindt, Wigner representation of Andreev-reflected charge pulses, [arXiv:2312.13829](#) (2025).
- [37] S. Vinjanampathy and J. Anders, Quantum thermodynamics, *Contemp. Phys.* **57**, 545 (2016).

## END MATTER

*Integrals*— For the electric current, we use that

$$\int_{-\infty}^{\infty} dx \frac{ia e^{iax}}{1 + e^x} = \frac{\pi a}{\sinh(\pi a)} = \chi(\pi a), \quad (11)$$

where  $a$  is a real constant, and we have defined the function  $\chi$ . For the heat current, we also need the integral

$$\int_{-\infty}^{\infty} dx \frac{a^2 x e^{iax}}{1 + e^x} = (\pi a)^2 \frac{\cosh(\pi a)}{\sinh^2(\pi a)} = \gamma(\pi a), \quad (12)$$

having defined the function  $\gamma$ . Both integrals can be found using contour integration in the complex plane.

*Gaussian pulses*— In the main text, we focus on Lorentzian voltage pulses, which have been realized in several experiments [7–9]. However, to connect with the numerical simulations of Ref. [22], which used Gaussian voltage pulses, we here consider a pulse of the form

$$V(t) = q \bar{V}_0 e^{-(t/t_0)^2} \quad (13)$$

where  $q$  is the emitted charge, and we have defined the width  $t_0 = \Gamma/\sqrt{\ln 2}$  and the prefactor  $\bar{V}_0 = 2\hbar\sqrt{\pi}/e t_0$ .

In Fig. 4, we show the electric current and the heat current generated by the pulses. The results in Fig. 4(a) agree well with the simulations in Ref. [22], and we see clear differences compared to the results in Fig. 2 for Lorentzian pulses. The inset shows how the negative currents are washed out by an increasing temperature. In Fig. 4(b), the heat current also turns negative.